

# A possible link between *KCNQ2*- and *STXBPI*-related encephalopathies: *STXBPI* reduces the inhibitory impact of syntaxin-1A on M current

\*Jérôme Devaux, †‡Sandra Dhifallah, †§Michela De Maria, †¶Geoffrey Stuart-Lopez, †Hélène Becq, #\*\*Mathieu Milh, †Florence Molinari, and †Laurent Aniksztejn

*Epilepsia*, \*\*(\*) :1–12, 2017

doi: 10.1111/epi.13927

## SUMMARY

**Objective:** Kv7 channels mediate the voltage-gated M-type potassium current. Reduction of M current due to *KCNQ2* mutations causes early onset epileptic encephalopathies (EOEEs). Mutations in *STXBPI* encoding the syntaxin binding protein I can produce a phenotype similar to that of *KCNQ2* mutations, suggesting a possible link between *STXBPI* and Kv7 channels. These channels are known to be modulated by syntaxin-1A (Syn-1A) that binds to the C-terminal domain of the Kv7.2 subunit and strongly inhibits M current. Here, we investigated whether *STXBPI* could prevent this inhibitory effect of Syn-1A and analyzed the consequences of two mutations in *STXBPI* associated with EOEEs.

**Methods:** Electrophysiologic analysis of M currents mediated by homomeric Kv7.2 or heteromeric Kv7.2/Kv7.3 channels in Chinese hamster ovary (CHO) cells coexpressing Syn-1A and/or *STXBPI* or mutants *STXBPI* p.W28\* and p.P480L. Expression and interaction of these different proteins have been investigated using biochemical and co-immunoprecipitation experiments.

**Results:** Syn-1A decreased M currents mediated by Kv7.2 or Kv7.2/Kv7.3 channels. *STXBPI* had no direct effects on M current but dampened the inhibition produced by Syn-1A by abrogating Syn-1A binding to Kv7 channels. The mutation p.W28\*, but not p.P480L, failed to rescue M current from Syn-1A inhibition. Biochemical analysis showed that unlike the mutation p.W28\*, the mutation p.P480L did not affect *STXBPI* expression and reduced the interaction of Syn-1A with Kv7 channels.

**Significance:** These data indicate that there is a functional link between *STXBPI* and Kv7 channels via Syn-1A, which may be important for regulating M-channel activity and neuronal excitability. They suggest also that a defect in Kv7 channel activity or regulation could be one of the consequences of some *STXBPI* mutations associated with EOEEs. Furthermore, our data reveal that *STXBPI* mutations associated with the Ohtahara syndrome do not necessarily result in protein haploinsufficiency.

**KEY WORDS:** Kv7 channels, M current, Syntaxin 1A, *STXBPI*, Early onset epileptic encephalopathies.



Jérôme Devaux is a CNRS researcher at Aix-Marseille University (France).

Accepted September 26, 2017.

\*CNRS, CRN2M-UMR7286, Aix-Marseille University, Marseille, France; †INSERM UMR\_S901, Mediterranean Neurobiology Institute (INMED), Aix-Marseille University, Marseille, France; ‡Institute of Molecular and Cellular Pharmacology (IPMC), CNRS, Nice Sophia-Antipolis University, Valbonne, France; §Department of Medicine and Health Sciences, University of Molise, Campobasso, Italy; ¶UMR5203 Institute of Functional Genomic (IGF), CNRS, Montpellier, France; #Timone Children Hospital, Pediatric Neurology department, APHM, Marseille, France; and \*\*GMGF, INSERM UMR\_S910, Aix-Marseille University, Marseille, France

Address correspondence to Laurent Aniksztejn, INMED-INSERM UMR\_S901, Parc Scientifique de Luminy, 13273 Marseille Cedex 09, France. E-mail: laurent.aniksztejn@inserm.fr

Wiley Periodicals, Inc.

© 2017 International League Against Epilepsy

## KEY POINTS

- Syntaxin-1A (Syn-1A) inhibits with same efficiency M current mediated by homomeric Kv7.2 and heteromeric Kv7.2/Kv7.3 channels in CHO cells
- STXBP1 does not affect M current but partially rescues M current from Syn-1A inhibition
- The mutant STXBP1 p.W28\* but not p.P480L associated with early onset epileptic encephalopathy (EOEE) does not restore M current
- The mutation p.W28\* but not p.P480L is deleterious for STXBP1 expression
- STXBP1 and the mutant STXBP1 p.P480L reduce the interaction of Syn-1A with Kv7 channels

Syntaxin-1A (Syn-1A) is a target plasma membrane SNARE protein (soluble *N*-ethylmaleimide-sensitive factor attachment protein receptor) that associates with other SNARE proteins (SNAP25, synaptobrevin) and with syntaxin binding protein 1 (STXBP1, a.k.a. Munc18.1) to form a complex that is instrumental for the docking of synaptic vesicles and their fusion with the plasma membrane for transmitter release.<sup>1</sup> Syn-1A also interacts with several ion channels and affects their expression and gating properties.<sup>2–4</sup> Notably, Syn-1A modulates the activity of Kv7 channels that mediates the slowly activating and non-inactivating voltage-gated potassium current called M current, which plays a major role in the control of neuronal excitability.<sup>3–7</sup> In many cortical neurons, these channels are composed by the homomeric assembly of Kv7.2 subunit and by the heteromeric assembly of Kv7.2 and Kv7.3 subunits.<sup>8–10</sup> Syn-1A binds on the helix A of the C-terminal domain of Kv7.2 and Kv7.3 subunits and facilitates the interaction between the N and C termini resulting in a decrease of the channel open probability.<sup>4</sup> However, Syn-1A exerts an inhibitory impact only on Kv7.2 channels, while it fails to inhibit current mediated by Kv7.3 channels due to differences in the N-terminal sequences of the two subunits.<sup>3,4</sup>

De novo mutations in the *KCNQ2* gene, which encodes for the Kv7.2 subunit, have been identified in early onset epileptic encephalopathies (EOEEs), and at least half of them with a suppression burst on electroencephalography (EEG) studies.<sup>11–13</sup> Functional analysis of mutant channels suggests that these diseases are caused mainly by a reduction of M current.<sup>14–16</sup> Along with *KCNQ2*, de novo mutations in the *STXBP1* gene have been described in >150 patients.<sup>17</sup> Most of these patients show severe encephalopathy with early onset epilepsy, and about 30–50% of them presented with an initial suppression-burst pattern on EEG.<sup>17–19</sup> The striking similarities in *STXBP1*- and *KCNQ2*-related disorders led us to investigate a possible biologic link between these conditions. It is of interest, STXBP1 has been shown to prevent the action of Syn-1A on

epithelial Na<sup>+</sup> and Cl<sup>−</sup> channels and voltage-gated N-type calcium channels.<sup>20–22</sup> We thus hypothesized that STXBP1 may reduce Syn-1A interaction with Kv7 channels, while mutant *STXBP1*-related encephalopathies may not. We tested this hypothesis using both electrophysiologic and biochemical approaches on homomeric Kv7.2 and heteromeric Kv7.2/Kv7.3 channels. We also analyzed the consequences of the nonsense mutation p.W28\* and of the missense mutation p.P480L in STXBP1 related to EOEEs without and with an initial suppression burst EEG pattern, respectively.<sup>19</sup>

## METHODS

### Molecular biology

Human coding DNAs (cDNAs) encoding STXBP1 (#NM\_001032221.3) and Syn-1A (#NM\_004603.1) were purchased from GeneCopoeia. Human cDNA encoding Kv7.2 (#NM\_172108.3) and Kv7.3 (#NM\_004519.3) were subcloned into pcDNA3.1 as previously described.<sup>16</sup> c.83G>A/p.28Trp>Stop and c.1439C>T/p.480Pro>Leu mutations (according to NM\_001032221.3) were introduced in the STXBP1 plasmids using the QuikChange II Site-Directed Mutagenesis Kit (Agilent), and mutation insertion was verified using Sanger sequencing (Table S1). For immunoprecipitation experiments, a Myc epitope was inserted at the intracellular N-terminal extremity of STXBP1.

### Cell culture and transfections

Chinese hamster ovary (CHO) cell culture conditions and transfections have already been described.<sup>16</sup> Briefly, 100,000 cells in suspension were transfected with a total amount of 1 μg of DNA containing a reporter plasmid with the GFP gene (0.2 μg) and cDNA constructs. Empty pcDNA3.1 was added if necessary, and concentrations were adjusted to get a total amount of 1 μg of DNA. Electroporation configuration was the following: 1,400 V, 1 pulse, 20 msec.

### Immunoprecipitation and Western blot

Cells expressing Kv7.2, Kv7.3, Syn-1A, and STXBP1 constructs were lysed for 15 min on ice in 1% Triton X-100, 140 mM NaCl, 20 mM Tris-HCl, and pH 7.4 containing protease inhibitors, and then centrifuged at 27,000 *g* for 30 min. The supernatants were saved and the protein concentrations were determined using the BCA kit (Sigma-Aldrich). Equal amounts of proteins were incubated overnight with the following antisera: a mouse antibody against Myc (Roche) or a rabbit antiserum against Kv7.2. Each sample was then incubated for 30 min at 4°C with a mixture of Protein A and G agarose beads (Sigma-Aldrich). After three washes with phosphate-buffered saline (PBS) plus 0.1% Triton X-100, 1% bovine serum albumin (BSA), and protease inhibitors, the bound proteins were released by

boiling in 20  $\mu$ l of sodium dodecyl sulfate (SDS) sample buffer for 2 min at 90°C. The released proteins were loaded on 7.5% sodium dodecyl sulfate polyacrylamide gel electrophoresis (SDS-PAGE) gels and transferred onto nitrocellulose membranes. The membranes were blocked for 1 h using 5% powdered skim milk in PBS with 0.5% Tween-20 and incubated with a rabbit antiserum against Kv7.2 (1/2,000),<sup>16</sup> a rabbit antiserum against Kv7.3 (1/2,000),<sup>16</sup> a mouse antibody against Syn-1A (1/2,000; Sigma-Aldrich), or a mouse antibody against Myc (1/2,000). After several washes, the blots were incubated with the appropriate peroxidase-coupled secondary antibodies (1/5,000; Jackson ImmunoResearch, West Grove, PA, U.S.A.) for 1 h and washed several times. Immunoreactivity was revealed using the BM chemiluminescence kit (Roche) and visualized on a G:BOX gel imaging and analysis system (Syngene, Cambridge, United Kingdom). The integrated densities of each protein band were measured with ImageJ software.

#### Cell biotinylation assay

The procedure used for cell biotinylation assay has been described previously.<sup>16</sup>

#### Electrophysiology

Cells were perfused at 1–2 ml/min with a solution of the following composition (in mM): 135 NaCl, 3.5 KCl, 5 NaHCO<sub>3</sub>, 0.5 NaH<sub>2</sub>PO<sub>4</sub>, 1 MgCl<sub>2</sub>, 1.5 CaCl<sub>2</sub>, 10 HEPES, 10 glucose, and pH 7.3 adjusted with NaOH. Whole-cell patch-clamp recordings were performed with microelectrodes (borosilicate glass capillaries GC150F-15, Harvard apparatus) filled with a solution containing (in mM): 135 KCl, 0.1 CaCl<sub>2</sub>, 1.1 ethylene glycol-bis(2-aminoethyl-ether)-N,N,N',N'-tetraacetic acid (EGTA), 10 4-(2-Hydroxyethyl) piperazine-1-ethanesulfonic acid (HEPES), 3 Mg<sup>2+</sup>ATP, 0.3Na<sup>+</sup>GTP, 4 phosphocreatinine, pH 7.3 adjusted with KOH, and a resistance of 4–6 M $\Omega$ . Data were sampled at 10 kHz and filtered with a cut-off frequency of 3 kHz using an EPC-10 amplifier (HEKA Elektronik). Voltage steps of 10 mV increment during 2 s from holding potential of –105 mV and up to +45 mV followed by a pulse to –65 mV for 1 s were applied to the cells to analyze the conductance/voltage (G/V) relationships and the kinetics of activation and deactivation of the channels. These series of voltage steps were performed once or twice for each cell. G values were obtained from peak amplitudes of the slow outward current divided by the driving force for K<sup>+</sup> ions with E<sub>K</sub>  $\sim$  –93 mV, a value close to that measured in our electrophysiologic recordings and normalized to the maximal conductance.

Plotted points were fitted with a Boltzmann function:  $G/G_{max} = 1/[1 + \exp(V_{1/2} - V_m)/k]$  to yield the voltage for half-maximum activation ( $V_{half}$ ) and the slope factor ( $k$ ) values. The procedure used to measure the channel kinetics has been described previously.<sup>16</sup> The current densities measured in cells coexpressing the channels (homo or

heteromeric), Syn-1A, and/or STXBPI were compared with the current densities of cells expressing only the channels. The values were first expressed in pA/pF and then normalized to the current density evoked at +45 mV by the homomeric Kv7.2 or heteromeric Kv7.2/Kv7.3 channels and recorded the same days as cells coexpressing the channels and proteins of interest. For each condition, this normalization was made to a quasi-equivalent number of cells expressing only the channels. Currents were analyzed using Origin 8.0 software. Analyses were performed after offline leak current subtraction. Membrane potentials were corrected for liquid junction potential ( $\sim$ 5 mV).

#### Statistics

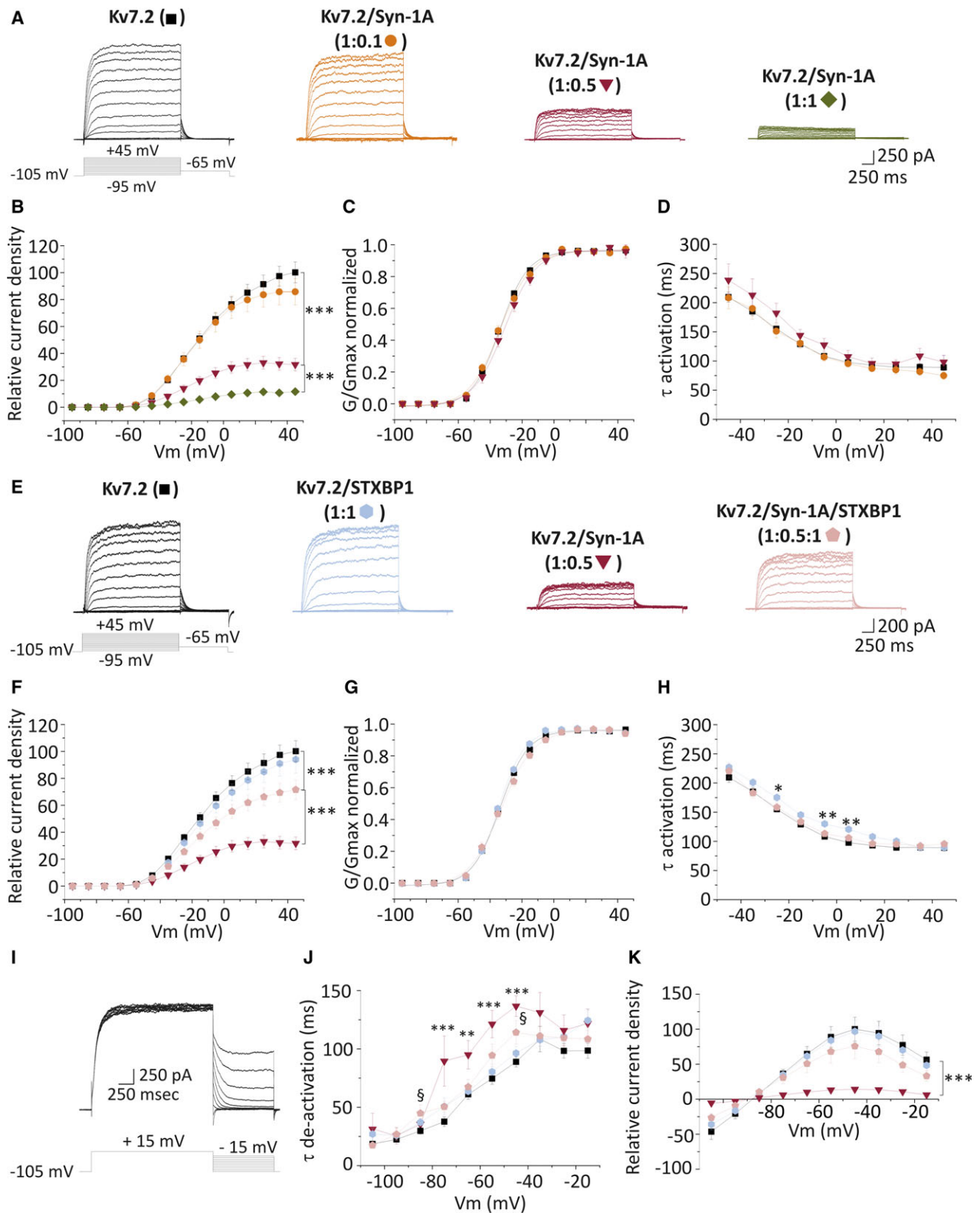
Data are represented as means  $\pm$  standard error of the mean (SEM). When the data's distribution was normal, we used a Student's *t*-test to compare means of two groups or the one-way analysis of variance (ANOVA) followed by Bonferroni's test as mentioned. When the normality test failed, we used the nonparametric Mann-Whitney test for two independent samples. Statistical analysis was performed using Graphpad Prism software. ns: not significant; \**p* < 0.05; \*\**p* < 0.01; and \*\*\**p* < 0.001.

## RESULTS

We first investigated whether CHO cells endogenously expressed genes encoding for Syn-1A or STXBPI by reverse transcriptase-polymerase chain reaction (RT-PCR). The amplified gene fragments were identical in size in both hamster and human (Table S2). No endogenous expression of these two genes was detected in CHO cells unless after transfection with cDNA encoding for the human proteins (Fig. S1). The same result was obtained for the *KCNQ2* gene. CHO cell lines thus appeared as a good model to test the effects of Syn-1A and STXBPI on M currents. We first examined the effects of Syn-1A on the current mediated by the homomeric Kv7.2 channels.

#### Syntaxin-1A decreased M current mediated by Kv7.2 in a “dose-dependent” manner

Depolarizing voltage steps applied from a holding membrane potential of –105 mV to +45 mV (10 mV increment) evoked a slowly activating outward current with a threshold potential of around –45 mV. The  $V_{half}$  and the K slope values were of  $-33 \pm 0.8$  mV and  $8.9 \pm 0.4$  mV/e-fold, respectively ( $n = 70$  cells; Fig. 1A and Table S3). Consistent with other studies, the activation kinetics were voltage sensitive with time constant decreasing with the depolarization.<sup>14–16</sup> The coexpression of Kv7.2 with increasing amounts of Syn-1A gradually reduced M current density. At +45 mV, M currents were reduced by nearly 15% with a 1:0.1 ratio ( $n = 8$  cells), by 70% and 90% when Syn-1A was transfected in a 1:0.5 ratio ( $n = 12$  cells) and 1:1 ratio,



respectively ( $n = 14$  cells; Fig. 1A,B and Table S3). This was not accompanied by a major change in the  $G/V$  relationship and activation kinetics (Fig. 1C,D and Table S3).

We next analyzed the impact of STXBP1 on M current in the absence or presence of Syn-1A. Expression of STXBP1 did not affect current density,  $G/V$  relationship, or

**Figure 1.**

Functional consequences of Syn-1A or/and STXBPI on current mediated by homomeric Kv7.2 channels. **(A)** Current responses to 10 mV incremental voltage step-command from  $-105$  mV to  $+45$  mV for 2 s followed by a 1 s hyperpolarizing voltage step to  $-65$  mV in CHO cells transfected with plasmids expressing Kv7.2 and Kv7.2 plus Syn-1A at ratio indicated in parenthesis. **(B)** Relative current density measured at all voltage steps showing the effects of coexpression with Syn-1A at the ratio indicated in parenthesis in **(A)** with the associated colored symbols. All values were normalized to the mean current density measured at  $+45$  mV in CHO expressing only the Kv7.2 subunit (see Methods). **(C–D)** Conductance–voltage (G/V) relationship and time constant of current activation in cells expressing Kv7.2 alone or in combination with Kv7.2 and Syn-1A at ratio of 1:0 and 1:0.5. Continuous lines in **(C)** represent Boltzmann fits to the experimental data. Measurement of these two parameters was not possible at ratio 1:1 because currents declined during the depolarizing voltage steps. **(E–H)** Functional consequences of STXBPI or STXBPI/Syn-1A coexpression on Kv7.2 current density **(F)**, G/V relationship **(G)**, and channel activation kinetics **(H)**. **(I)** Tail currents observed after a 1 s hyperpolarizing voltage step command from  $+15$  mV to membrane potentials ranging from  $-15$  mV to  $-105$  mV. **(J)** Weight average time constant of current deactivation and **(K)** relative tail current density were measured in cells expressing Kv7.2 only ( $n = 25$  cells) or coexpressing Kv7.2/Syn-1A ( $n = 7$  cells), Kv7.2/STXBPI ( $n = 24$  cells), Kv7.2/Syn-1A/STXBPI ( $n = 7$  cells) at ratio indicated in parenthesis in **(E)**.

*Epilepsia* © ILAE

activation and deactivation time constants ( $n = 41$  cells; Fig. 1F–H and Table S3).

The co-transfection of Kv7.2 and Syn-1A with STXBPI at a 1:0.5:1 ratio ( $n = 21$  cells) dampened the inhibitory impact of Syn-1A on current density, leading to a current reduction of only 30% (meaning a current recovery of 40%; Fig. 1F). The recovery was also observed when measuring the tail current density (Fig. 1K). Moreover, STXBPI abolished the effects of Syn-1A on current deactivation that was slowed at a 1:0.5 ratio (Fig. 1J). STXBPI also significantly reduced the impact of Syn-1A on current density by 25% when co-transfected with a ratio of 1:1:1 ( $n = 7$  cells; graph not shown, see also Table S3).

### Heteromeric Kv7.2/Kv7.3 channels are modulated by Syn-1A

Previous observations performed in *Xenopus* oocytes have shown that Kv7.2/Kv7.3 channels are less sensitive to Syn-1A than homomeric Kv7.2 channels, likely because Kv7.3 subunits are not sensitive to Syn-1A.<sup>3,4</sup> We reinvestigated this issue in CHO cells and found that increasing amounts of Syn-1A reduced current densities by 45% (1:1:0.25 ratio,  $n = 13$  cells), 62% (1:1:0.5 ratio,  $n = 28$  cells), and 80% (1:1:1 ratio  $n = 6$  cells) at  $+45$  mV (Fig. 2A,B). The percentage of decrease for the two last configurations were not significantly different from values obtained with the homomeric Kv7.2 channels, indicating that the heteromerization did not alter the sensitivity of the channels to Syn-1A. Syn-1A also slowed the activation time constant of M current when expressed at a 1:1:1 ratio but not at lower ratios (Fig. 2D). Syn-1A did not have major consequences on the channel deactivation time constant and G/V relationship, although a slight but significant decrease of the slope factor was observed (Fig. 2C,F and Table S3).

### STXBPI reduced the inhibitory impact of Syn-1A on heteromeric Kv7.2/Kv7.3 channels

As for homomeric Kv7.2 channels, STXBPI did not affect the characteristics of the heteromeric current but its

expression reduced the inhibitory impact of Syn-1A. The recovery of current densities measured at  $+45$  mV was of 35% and 25% at 1:1:0.5:1 and 1:1:1:1 ratios ( $n = 16$  and 7 cells, respectively, Fig. 2F,G and Table S3). Moreover, STXBPI restored the activation channel kinetics (Fig. 2H). Together, these data indicated that STXBPI modulates the functional effect of Syn-1A on Kv7 channels.

### Differential effects of two mutations in STXBPI related to early onset epileptic encephalopathy

Because mutations in *STXBPI* have been identified in patients with EOEE, we investigated the effects of two mutations on M current. The mutation p.W28\* is a nonsense mutation identified in a patient with a nonsyndromic EOEE<sup>19</sup> without an initial suppression burst at the EEG resulting in premature stop codon at position 28 within the D1 domain of the protein. The second mutation p.P480L is a missense mutation localized in the D3 domain of the protein where the proline in position 480 is replaced by a leucine. This mutation has been identified in a patient with Ohtahara syndrome.<sup>19</sup>

These two mutant proteins did not affect the density of M current mediated by the heteromeric Kv7.2/Kv7.3 channels (Fig. 3A,B and Table S3) but differentially modulated the effects of Syn-1A. Thus STXBPI p.W28\* failed to reduce the inhibitory impact of Syn-1A on heteromeric channels ( $n = 21$  cells). In contrast, STXBPI p.P480L rescued current density to a level that was not significantly different from what was observed with wild-type STXBPI ( $n = 17$  cells; Fig. 3C,D and Table S3).

We then performed Western blot and co-immunoprecipitation experiments to understand the differential effects of the two mutants and the mechanisms by which STXBPI neutralized the action of Syn-1A. Different mechanisms could account for the action of STXBPI including an effect on Kv7 channel expression and trafficking; a reduced expression of Syn-1A; the formation of a complex STXBPI/Syn-1A/Kv7 channels; and a reduced interaction of Syn-1A with the subunits.

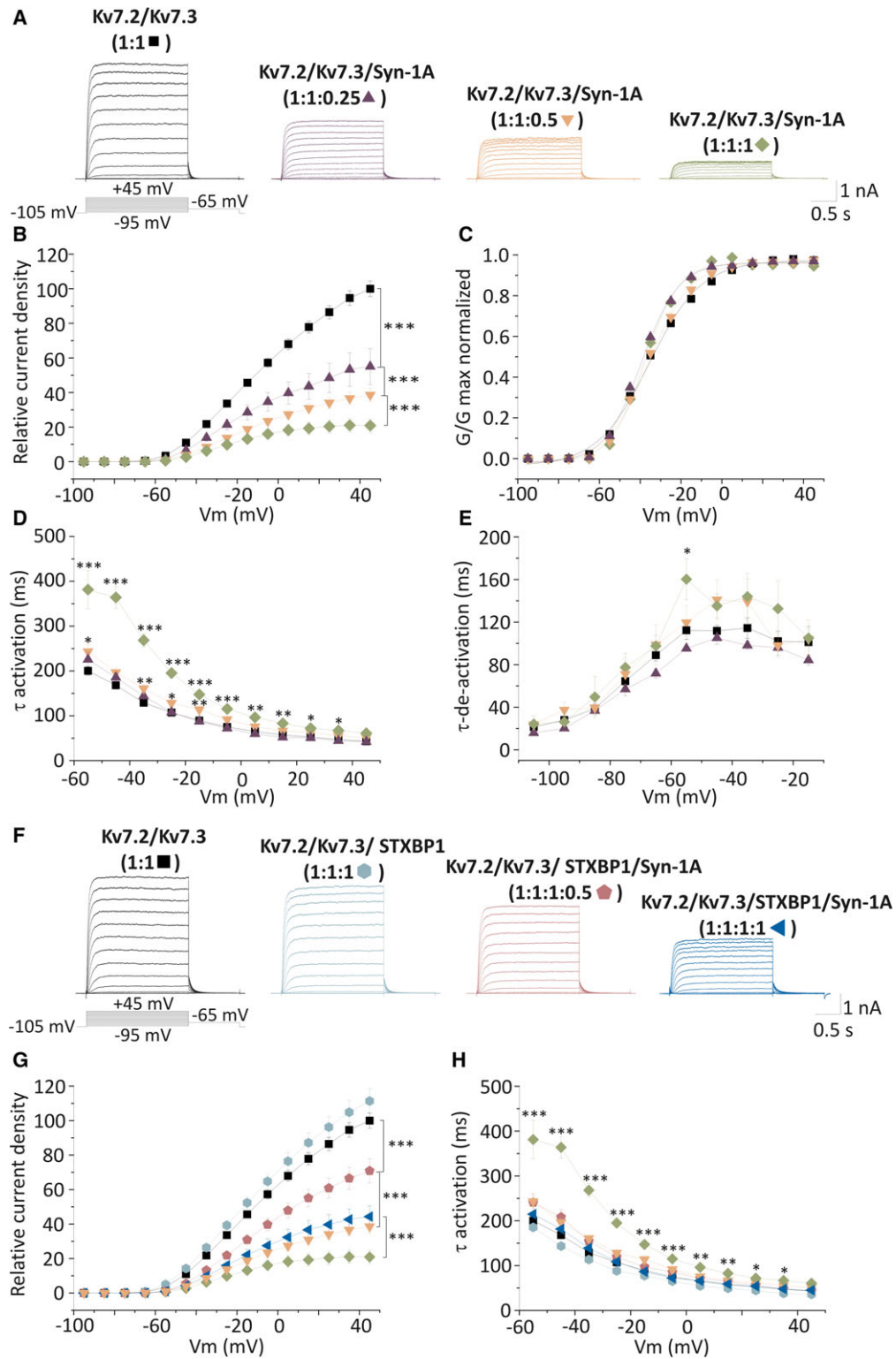


**Figure 2.**

Functional consequences of Syn-1A and STXBPI on current mediated by heteromeric Kv7.2/Kv7.3 channels. **(A)** Current responses to depolarizing voltage steps of Kv7.2/Kv7.3 or Kv7.2/Kv7.3/Syn-1A at ratio indicated in parenthesis. **(B–E)** Functional consequences of Syn-1A coexpression on Kv7.2/Kv7.3 current density **(B)**, G/V relationship **(C)**, time constant of current activation **(D)**, and deactivation **(E)**. **(F–H)** Functional consequences of STXBPI or STXBPI/Syn-1A coexpression on Kv7.2/Kv7.3 current density **(G)** and channel activation kinetics **(H)**.

*Epilepsia* © ILAE

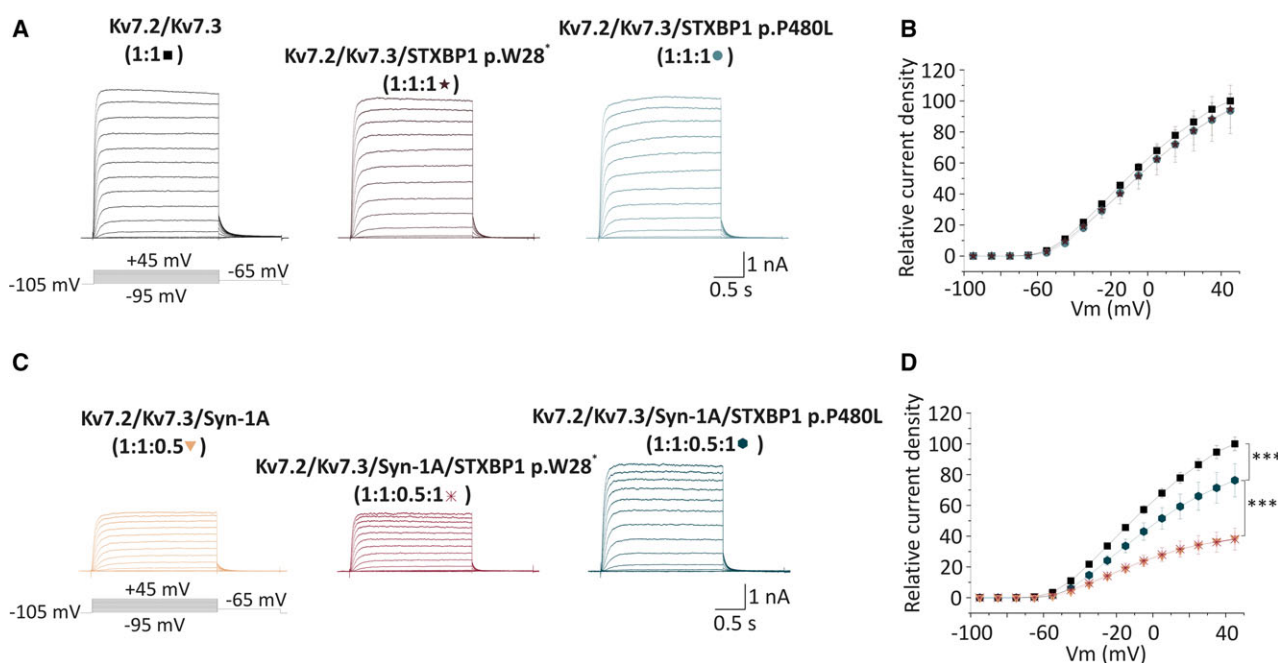


**Figure 3.**

Functional consequences of *STXBP1* mutations p.W28\* and p.P480L on current mediated by Kv7.2/Kv7.3 channels. **(A–B)** Kv7.2/Kv7.3 currents were evoked by depolarizing voltage steps **(A)** and relative current density **(B)** were measured in absence or presence of *STXBP1* p.W28\* and p.P480L. **(C–D)** Cells were co-transfected with Syn-1A, and currents were evoked by depolarizing voltage steps **(C)** and the relative current density **(D)** were measured in absence or presence of *STXBP1* p.W28\* and p.P480L.

*Epilepsia* © ILAE

### STXBP1 interaction with Syn-1A is impaired by STXBP1 p.W28\* but not by p.P480L mutation

We first analyzed the consequences of the mutations on both *STXBP1* expression and on Syn-1A levels and then on *STXBP1*/Syn-1A interaction. To detect the mutant proteins and perform pull-down experiments, a Myc epitope was inserted at the N-terminus of *STXBP1*. Cells were co-transfected with Syn-1A and wild-type or mutant *STXBP1*, and *STXBP1* was pulled down with a monoclonal anti-Myc antibody (Fig. 4A). As expected, wild-type *STXBP1* interacted with Syn-1A. The mutation p.W28\* severely impacted the expression of the mutant protein and thus lacked interaction with Syn-1A. By contrast, the expression of *STXBP1* was not affected by the mutation p.P480L (Fig. 4B). Nevertheless, its interaction with Syn-1A was significantly decreased compared to wild-type *STXBP1*. The expression of Syn-1A was not changed following co-transfection with wild-type or mutant *STXBP1*, indicating that Syn-1A stability is not dependent on *STXBP1*.

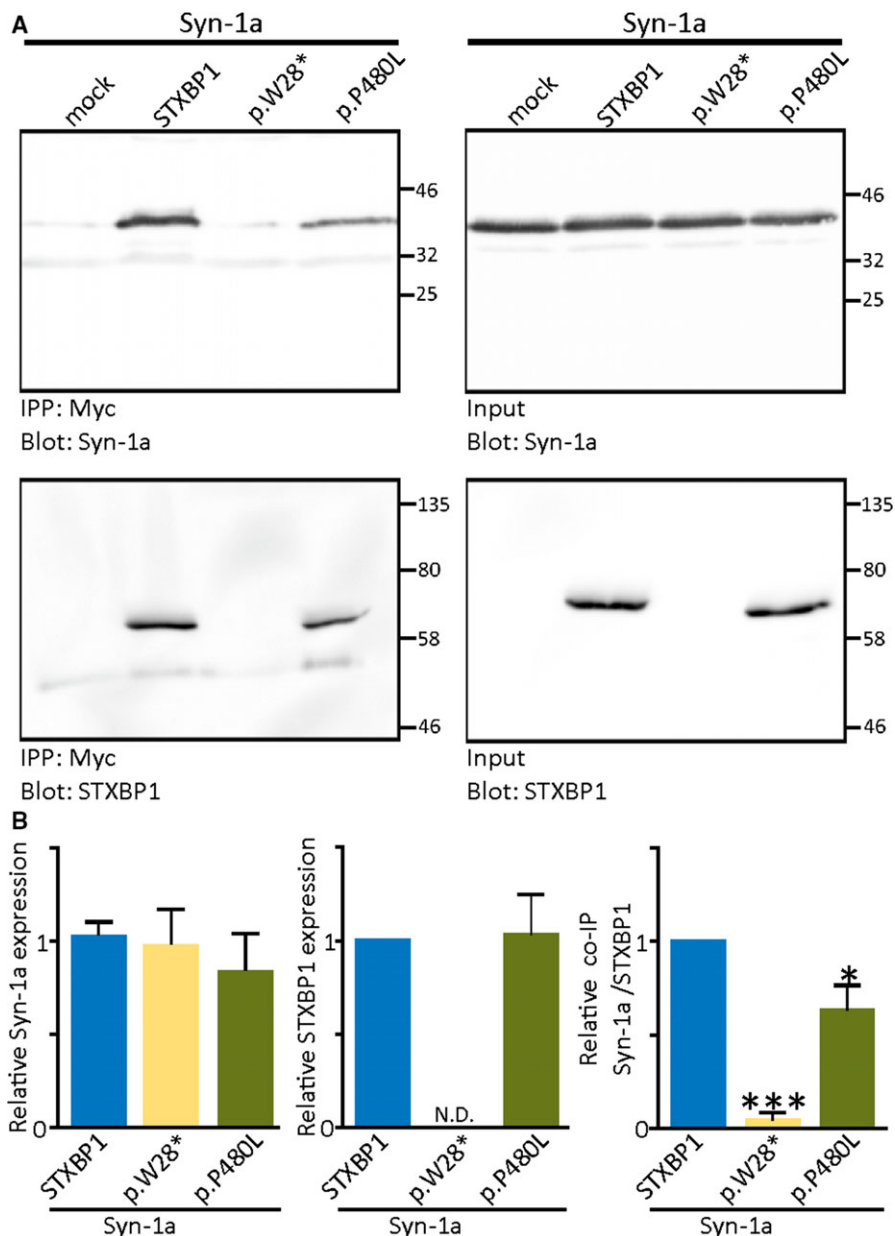
### Syn-1A and STXBP1 did not modulate the membrane trafficking of Kv7.2/Kv7.3 channels

We examined whether Syn-1A, *STXBP1*, or both proteins affected the total and surface expression of Kv7.2 and Kv7.3 subunits. Syn-1A, but not *STXBP1*, increased the total expression of Kv7.2/Kv7.3 subunits (Figs. S2 and S3). The effect of Syn-1A was prevented when co-expressed

with *STXBP1* (Fig. S2). However, the surface expression of both subunits was not significantly different in the presence of Syn-1A and/or *STXBP1*, indicating that these proteins do not regulate membrane channel trafficking. Therefore, the recovery of M current observed in presence of *STXBP1* did not result from an increase in membrane expression of Kv7 channels.

### STXBP1 modulates association of Syn-1A with Kv7.2/Kv7.3 channels

Because Syn-1A is known to interact with Kv7 channels, we thus hypothesized that *STXBP1* may act by reducing the interaction of Syn-1A with Kv7 channels. For that purpose, Kv7.2/Kv7.3 subunits were co-transfected with Syn-1A in the presence or absence of Myc-tagged *STXBP1* constructs, and Kv7.2/Kv7.3 channels were pulled down with a polyclonal antibody against Kv7.2 (Fig. 5A). In keeping with previous reports,<sup>3</sup> Syn-1A was found to associate with Kv7.2/Kv7.3 channels (Fig. 5A). This interaction was strongly impaired by the presence of wild-type *STXBP1* or p.P480L mutant, but not by the p.W28\* mutant (Fig. 5B). Of interest, we did not detect any interaction between Kv7.2/Kv7.3 channels and wild-type or mutant *STXBP1*. As controls, we examined the association of Kv7.2 subunits with Kv7.3. The channel heteromerization was not impacted by the presence of Syn-1A, *STXBP1*, or both (Fig. 5B).

**Figure 4.**

*STXBPI* mutations affect the interaction of *STXBPI* with *Syn-1A*. **(A)** *Syn-1A* was expressed in combination with wild-type or mutant forms of Myc-tagged *STXBPI*. As a negative control, *Syn-1A* was expressed with an empty plasmid (mock). Cell lysates were immunoprecipitated for Myc and immunoblotted for *STXBPI* and *Syn-1A*. Total cell lysates (input) were immunoblotted for *STXBPI* and *Syn-1A*. Wild-type *STXBPI* co-immunoprecipitated with *Syn-1A*. Note that p.W28\* and p.P480L mutations affected the interaction with *Syn-1A*. The immunoglobulin (Ig) bands are indicated with an arrowhead. Molecular weight markers are shown on the right (in kDa). **(B)** Relative expressions were quantified by measuring the ratio of total *Syn-1A* or *STXBPI* relative to that of actin. The expression of *Syn-1A* was normalized to the mock condition, whereas the expression of mutant *STXBPI* was normalized to that of wild-type *STXBPI* ( $n = 4$  independent experiments). The interaction with *Syn-1A* was quantified by measuring the ratio of immunoprecipitated *Syn-1A*/immunoprecipitated *STXBPI*. Ratios were then normalized to those of wild-type *STXBPI* ( $n = 4$  independent experiments). p.W28\* and p.P480L mutations had no significant consequences on protein levels but significantly decreased *Syn-1A*/*STXBPI* interaction.

*Epilepsia* © ILAE

## DISCUSSION

*STXBPI*- and *KCNQ2*-related encephalopathies share some common features, including a neonatal-onset epilepsy

with a suppression-burst EEG pattern in 30–50% of patients, the evolution of epilepsy with an overall reduction of seizures but with persistence of severe mental

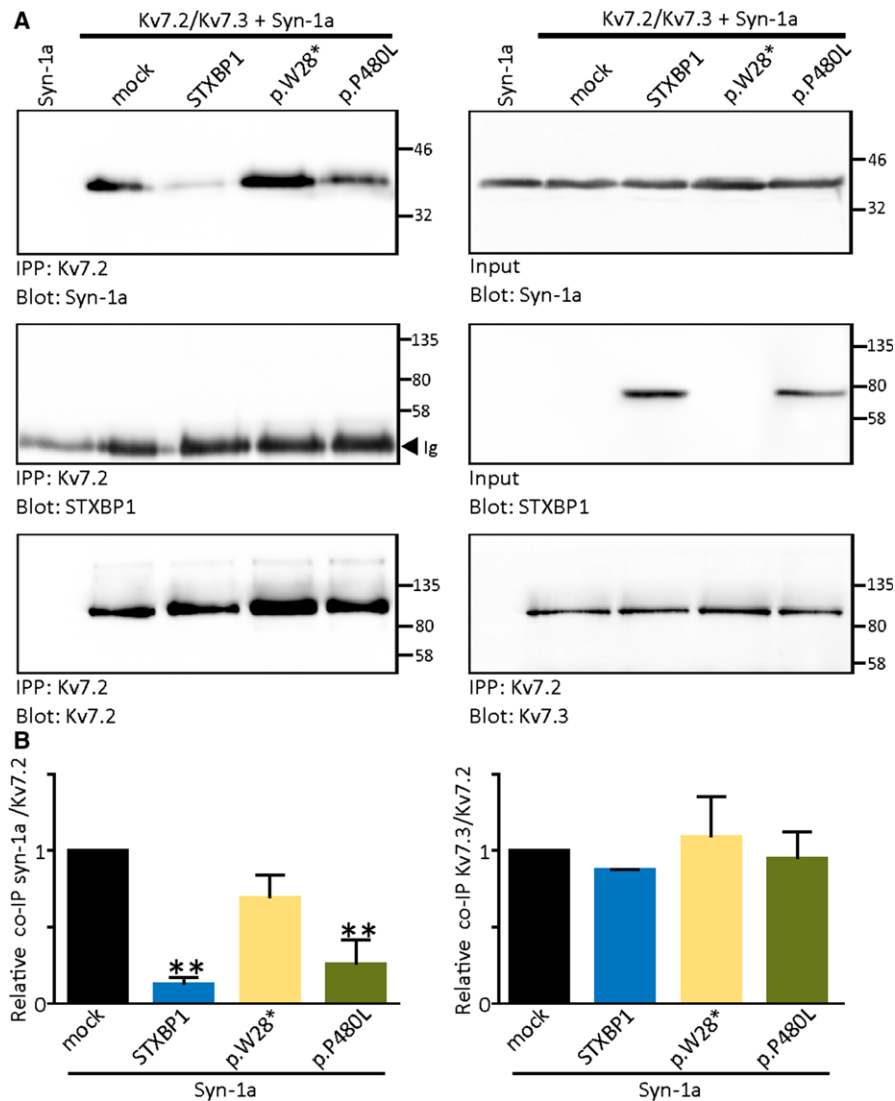


**Figure 5.**

STXBP1 modulates the association between Syn-1A and heteromeric Kv7.2/Kv7.3 channels. **(A)** Kv7.2/Kv7.3 subunits were coexpressed with Syn-1A and an empty plasmid (mock) or in combination with the wild-type or mutant forms of STXBP1. As negative controls, cells were transfected with Syn-1A alone. Cell lysates were immunoprecipitated for Kv7.2 and immunoblotted for Syn-1A, STXBP1, Kv7.2, and Kv7.3. Total cell lysates (input) were immunoblotted for Syn-1A and STXBP1. The results show that Kv7.2/Kv7.3 co-immunoprecipitated with Syn-1A. The coexpression of STXBP1 almost abolished the association of Syn-1A with Kv7.2/Kv7.3. The p.W28\* mutation, but not p.P480L mutation, impaired the effect of STXBP1 on Kv7.2/Kv7.3/Syn-1A interaction. Wild-type or mutant STXBP1 forms did not affect Kv7.2/Kv7.3 association and did not interact with Kv7.2/Kv7.3. The Ig bands are indicated with an arrowhead. Molecular weight markers are shown on the right (in kDa). **(B)** Relative interactions with Syn-1A or Kv7.3 were quantified by measuring the ratio of immunoprecipitated Syn-1A or Kv7.3/immunoprecipitated Kv7.2. Ratios were then normalized to the mock condition ( $n = 4$  independent experiments). The wild-type and p.P480L forms, but not p.W28\*, significantly decreased the association of Kv7.2/Kv7.3 with Syn-1A.

Epilepsia © ILAE

retardation.<sup>11,12,17–19</sup> We have established here that a link could exist between STXBP1 and Kv7 channels.

We provide evidence that STXBP1 reduces the interaction of Syn-1A with Kv7 channels and partially counterbalances the inhibitory impact of Syn-1A on M current. This effect of STXBP1 could theoretically occur in neurons

according to immunohistochemical studies showing that STXBP1 distribution parallels that of Syn-1A and of Kv7 channels throughout the axon and synaptic terminals.<sup>9,23–27</sup> Therefore, although STXBP1 does not bind to Kv7 channels, its expression may contribute to ensure the proper function of Kv7 channels. A previous study suggests that

calmodulin could play this role but depending on its concentration and its ability to associate with calcium it can also exert an inhibitory impact that is additive to the Syn-1A effect.<sup>4</sup>

The fact that the mutant p.W28\* could not reverse the effect of Syn-1A raised the possibility that the reduced expression of STXBPI encountered in *STXBPI*-related epileptic encephalopathies<sup>18,28</sup> may lead to an increased interaction between Syn-1A and Kv7 channels and potentially between syn-1A and its other partners.<sup>2</sup> Nonetheless, the lower impact of the p.P480L mutation indicates that this hypothesis cannot be generalized to all *STXBPI* mutations and therefore that the relationship between *STXBPI* mutations and EOEE is complex and may implicate several different mechanisms.

In keeping with previous works performed in *Xenopus* oocytes,<sup>3,4</sup> we showed in CHO cells that M currents are highly sensitive to Syn-1A. However, in contrast with these studies we found that Syn-1A affected similarly homomeric Kv7.2 and heteromeric Kv7.2/Kv7.3 channels. A strong sensitivity of Kv7.2/Kv7.3 channels to Syn-1A has also been noticed by Soldovieri and colleagues (2014)<sup>29</sup> using CHO cells. This discrepancy could be inherent to the experimental procedure. Notably, the use of Kv7.3 bearing the p.A315T mutation may have led to an underestimation of the effects of Syn-1A on heteromeric channels.<sup>3</sup> Because Syn-1A appears to affect similarly homomeric and heteromeric channels, this suggests that Syn-1A could endogenously inhibit M current in cortical cells where heteromeric Kv7.2/Kv7.3 channels predominate.<sup>8,9</sup>

The observation that Syn-1A increased total Kv7 channels expression was unexpected and has not been reported in *Xenopus* oocytes.<sup>3,4</sup> These data are opposite to the action of Syn-1A on current density and reveal the powerful inhibitory effect of Syn-1A on channel gating that is not compensated by the overall increased expression of the channels. This suggests that in mammalian cells, Syn-1A may either increase channel synthesis or may reduce the degradation/turnover of the subunits. Our data indicate also that Syn-1A did not affect Kv7 channel trafficking. This is not the case for the Kv1.1, Kv2.1, Kv4.2, or ENac, an amiloride sensitive-epithelial Na<sup>+</sup> channels that are modulated by Syn-1A via a decrease in their expression at plasma membrane.<sup>21,30–32</sup> This denotes the large repertoire of action of Syn-1A that can regulate ionic channel activity by a direct effect on the gating properties and/or indirectly by an effect on channels trafficking.<sup>2</sup>

The use of mutant forms of STXBPI showing different potencies to bind Syn-1A confirmed the effects of wild-type STXBPI. STXBPI p.W28\* that deleteriously affected STXBPI protein expression did not modulate the effects of Syn-1A, whereas Syn-1A inhibition was similarly reversed by wild-type STXBPI or STXBPI p.P480L which presented a correct expression and interaction with Syn-1A. It

is notable that STXBPI effects appeared partial with a recovery of current density that was around 30–40%. This differs from the results of other studies in which STXBPI fully rescued epithelial chloride and sodium currents from Syn-1A inhibition.<sup>20,21</sup> There are at least two possible explanations for the partial recovery observed in the present study. First, Syn-1A may associate with the Kv7 subunits with higher affinity than with other ion channels, thus requiring higher amounts of free STXBPI. Second, Syn-1A could interact with Kv7 channels in both open and closed forms (the N-terminal Habc domain folds back onto the C-terminal SNARE motif of the protein). Free Syn-1A exhibits a rapid dynamic equilibrium between the closed and open forms,<sup>33</sup> and both conformations of Syn-1A have been shown to modulate the Kv2.1 channels, the open form having even a more powerful inhibitory impact on current amplitude.<sup>34</sup> However, STXBPI forms a complex with Syn-1A when the latter is in closed conformation.<sup>27</sup> Thus it is possible that STXBPI alleviates the inhibition mediated by the closed form of Syn-1A, leaving the interaction between Kv7 channels and the open form of Syn-1A. In keeping with this, we found that STXBPI strongly decreased the interaction of Syn-1A with Kv7.2/Kv7.3, but a residual Syn-1A binding could still be detected.

Our biochemical data suggest that STXBPI rescues the current density by preventing the association of Syn-1A with Kv7 subunit and not by inducing a reduction of Syn-1A levels, since its relative expression was not affected by STXBPI or mutant proteins. The following two potential mechanisms could explain the inhibition of Syn-1A/Kv7 channel interaction by STXBPI: (1) the configuration adopted by STXBPI-Syn-1A dimer does not allow Syn-1A to bind to the C-terminal domain of Kv7.2/Kv7.3 subunits; or (2) STXBPI and Kv7 channels share the same site of interaction on Syn-1A. In the latter case, this would indicate that the effect of Syn-1A is mediated by the N-terminal Habc domain of the protein to which STXBPI binds. However, this domain does not seem to be the primary site associating with ion channels. Several studies indicate that the H3 domain of Syn-1A is the critical motif mediating the binding and modulation of epithelial sodium channel, ATP-dependent potassium channels, Kv2.1, Kv4.2 and N-type calcium channels.<sup>2,34–36</sup> Further studies are needed to clarify the molecular determinant that governs the action of Syn-1A and STXBPI on Kv7 channels.

Our data showed that the missense mutation p.P480L identified in a patient with Ohtahara syndrome did not lead to a degradation of the protein. Therefore, this syndrome is not necessarily caused by *STXBPI* haploinsufficiency as it was suggested in other studies.<sup>18,28</sup> It is difficult to understand how this mutant can cause epileptic encephalopathy and induce the same phenotype as other mutations reported to disrupt the conformation of the protein.<sup>37</sup> Moreover, the mutant p.P480L protein appeared to retain its capacity to complex with Syn-1A and showed functional effects on M

current comparable to that of wild-type STXBPI. It is possible that the decreased Syn-1A/STXBPI p.P480L interaction weakens dimer formation and subsequently their association with other proteins involved in the formation of the SNARE complex.

Finally, our data increase the knowledge on the pathophysiological consequences of STXBPI dysregulation. It has recently been shown that a mutation inducing a reduction of STXBPI expression decreases both evoked glutamate receptor-mediated synaptic transmission and expression of Syn-1A<sup>28,38</sup> (but see Toonen and colleagues<sup>39,40</sup>). This induced also the mislocalization of Syn-1A and impaired neurite outgrowth in patient pluripotent-derived neuronal cells.<sup>28</sup> Our data suggest that STXBPI mutations can indirectly affect the function of Kv7 channels. This may be true for other channels containing binding sites for Syn-1A. Thus channelopathies should also be considered in the pathogenicity of *STXBPI* mutations. Future studies performed in neurons inactivated for Syn-1A, STXBPI, or expressing *STXBPI* mutations are needed to confirm that Kv7 channels and firing properties are endogenously regulated by these proteins. This is important as it should open new therapeutic strategies for *STXBPI*-related conditions.

## ACKNOWLEDGMENTS

This work was supported by the Agence National pour la Recherche (ANR -14-CE13-0011-02, EPIK), ERA-Net for Research on Rare Diseases (ANR-13-RARE-0001-01; JD), and the Association Française contre les Myopathies (MNM1 2012-14580; JD). This work was also supported by INSERM, CNRS, Programme Hospitalier de Recherche Clinique (PHRC), and Aix-Marseille University.

## DISCLOSURE

None of the authors has any conflict of interest to disclose. We confirm that we have read the Journal's position on issues involved in ethical publication and affirm that this report is consistent with those guidelines.

## REFERENCES

- Südhof TC. The molecular machinery of neurotransmitter release (Nobel lecture). *Angew Chem Int Ed Engl* 2014;53:12696–12717.
- Leung YM, Kwan EP, Ng B, et al. SNAREing voltage-gated K<sup>+</sup> and ATP-sensitive K<sup>+</sup> channels: tuning beta-cell excitability with syntaxin-1A and other exocytotic proteins. *Endocr Rev* 2007;28:653–663.
- Regev N, Degani-Katzav N, Korngreen A, et al. Selective interaction of syntaxin 1A with KCNQ2: possible implications for specific modulation of presynaptic activity. *PLoS ONE* 2009;4:e6586.
- Etzioni A, Siloni S, Chikvashvili D, et al. Regulation of neuronal M-channel gating in an isoform-specific manner: functional interplay between calmodulin and syntaxin 1A. *J Neurosci* 2011;31:14158–14171.
- Jentsch TJ. Neuronal KCNQ potassium channels: physiology and role in disease. *Nat Rev Neurosci* 2000;1:21–30.
- Yue C, Yaari Y. Axo-somatic and apical dendritic Kv7/M channels differentially regulate the intrinsic excitability of adult rat CA1 pyramidal cells. *J Neurophysiol* 2006;95:3480–3495.
- Shah MM, Migliore M, Valencia I, et al. Functional significance of axonal Kv7 channels in hippocampal pyramidal neurons. *Proc Natl Acad Sci USA* 2008;105:7869–7874.
- Wang HS, Pan Z, Shi W, et al. KCNQ2 and KCNQ3 potassium channel subunits: molecular correlates of the M-channel. *Science* 1998;282:1890–1893.
- Battefeld A, Tran BT, Gavrilis J, et al. Heteromeric Kv7.2/7.3 channels differentially regulate action potential initiation and conduction in neocortical myelinated axons. *J Neurosci* 2014;34:3719–3732.
- Soh H, Pant R, LoTurco JJ, et al. Conditional deletions of epilepsy-associated KCNQ2 and KCNQ3 channels from cerebral cortex cause differential effects on neuronal excitability. *J Neurosci* 2014;34:5311–5321.
- Weckhuysen S, Mandelstam S, Suls A, et al. KCNQ2 encephalopathy: emerging phenotype of a neonatal epileptic encephalopathy. *Ann Neurol* 2012;7:15–25.
- Milh M, Boutry-Kryza N, Sutera-Sardo J, et al. Similar early characteristics but variable neurological outcome of patients with a *de novo* mutation of KCNQ2. *Orphanet J Rare Dis* 2013;8:80.
- Miceli F, Soldovieri MV, Joshi N, et al. KCNQ2-related disorders. In Adam MP, et al. (Eds) *GeneReviews*® [Internet]. Seattle (WA): University of Washington, Seattle; 2010 [updated 2016 Mar 31].
- Miceli F, Soldovieri MV, Ambrosino P, et al. Genotype-phenotype correlations in neonatal epilepsies caused by mutations in the voltage sensor of K(v)7.2 potassium channel subunits. *Proc Natl Acad Sci USA* 2013;110:4386–4391.
- Orhan G, Bock M, Schepers D, et al. Dominant-negative effects of KCNQ2 mutations are associated with epileptic encephalopathy. *Ann Neurol* 2014;75:382–394.
- Abidi A, Devaux J, Molinari F, et al. A recurrent KCNQ2 pore mutation causing early onset epileptic encephalopathy has a moderate effect on M current but alters subcellular localization of Kv7 channels. *Neurobiol Dis* 2015;80:80–92.
- Stamberger H, Nikanorova M, Willemsen MH, et al. STXBPI encephalopathy: a neurodevelopmental disorder including epilepsy. *Neurology* 2016;86:954–962.
- Saitu H, Kato M, Mizuguchi T, et al. De novo mutations in the gene encoding STXBPI (MUNC18-1) cause early infantile epileptic encephalopathy. *Nat Genet* 2008;40:782–788.
- Di Meglio C, Lesca G, Villeneuve N, et al. Epileptic patients with de novo STXBPI mutations: key clinical features based on 24 cases. *Epilepsia* 2015;56:1931–1940.
- Naren AP, Nelson DJ, Xie W, et al. Regulation of CFTR chloride channels by syntaxin and Munc18 isoforms. *Nature* 1997;390:302–305.
- Qi J, Peters KW, Liu C, et al. Regulation of the amiloride-sensitive epithelial sodium channel by syntaxin1A. *J Biol Chem* 1999;274:30345–30348.
- Gladysheva SE, Ho CS, Lee YY, et al. Regulation of syntaxin1A-munc18 complex for SNARE pairing in HEK293 cells. *J Physiol* 2004;558:857–871.
- Garcia EP, McPherson PS, Chilcote TJ, et al. rbSec1A and B colocalize with syntaxin 1 and SNAP-25 throughout the axon, but are not in a stable complex with syntaxin. *J Cell Biol* 1995;129:105–120.
- Devaux JJ, Kleopa KA, Cooper EC, et al. KCNQ2 is a nodal K<sup>+</sup> channel. *J Neurosci* 2004;24:1236–1244.
- Pan Z, Kao T, Horvath Z, et al. A common ankyrin-G-based mechanism retains KCNQ and NaV channels at electrically active domains of the axon. *J Neurosci* 2006;26:2599–2613.
- Rasmussen HB, Frøkjær-Jensen C, Jensen CS, et al. Requirement of subunit co-assembly and ankyrin-G for M-channel localization at the axon initial segment. *J Cell Sci* 2007;120:953–963.
- Toonen RF, Verhage M. Munc18-1 in secretion: lonely Munc joins SNARE team and takes control. *Trends Neurosci* 2007;30:564–572.
- Yamashita S, Chiyonobu T, Yoshida M, et al. Mislocalization of syntaxin-1 and impaired neurite growth observed in a human iPSC model for STXBPI-related epileptic encephalopathy. *Epilepsia* 2016;57:e81–e86.
- Soldovieri MV, Boutry-Kryza N, Milh M, et al. Novel KCNQ2 and KCNQ3 mutations in a large cohort of families with benign neonatal epilepsy: first evidence for an altered channel regulation by syntaxin-1A. *Hum Mutat* 2014;35:356–367.
- Fili O, Michaelevski I, Bledi Y, et al. Direct interaction of a brain voltage-gated K<sup>+</sup> channel with syntaxin 1A: functional impact on channel gating. *J Neurosci* 2001;21:1964–1974.

31. Leung YM, Kang Y, Gao X, et al. Syntaxin 1A binds to the cytoplasmic C terminus of Kv2.1 to regulate channel gating and trafficking. *J Biol Chem* 2003;278:17532–17538.
32. Yamakawa T, Saith S, Li Y, et al. Interaction of syntaxin 1A with the N-terminus of Kv4.2 modulates channel surface expression and gating. *Biochemistry* 2007;46:10942–10949.
33. Margittai M, Widengren J, Schweinberger E, et al. Single-molecule fluorescence resonance energy transfer reveals a dynamic equilibrium between closed and open conformations of syntaxin 1. *Proc Natl Acad Sci USA* 2003;100:15516–15521.
34. Leung YM, Kang Y, Xia F, et al. Open form of syntaxin-1A is a more potent inhibitor than wild-type syntaxin-1A of Kv2.1 channels. *Biochem J* 2005;387:195–202.
35. Bezprozvanny I, Zhong P, Scheller RH, et al. Molecular determinants of the functional interaction between syntaxin and N-type Ca<sup>2+</sup> channel gating. *Proc Natl Acad Sci USA* 2000;97:13943–13948.
36. Condliffe SB, Carattino MD, Frizzell RA, et al. Syntaxin 1A regulates ENaC via domain-specific interactions. *J Biol Chem* 2003;278:12796–12804.
37. Saitsu H, Kato M, Matsumoto N. Haploinsufficiency of STXBPI and Ohtahara syndrome. In Nobels JL, et al. (Eds) *Jasper's basic mechanisms of the epilepsies*. 4th Ed. Bethesda (MD): National Center for Biotechnology Information (US); 2012:1–11.
38. Patzke C, Han Y, Covy J, et al. Analysis of conditional heterozygous STXBPI mutations in human neurons. *J Clin Invest* 2015;125:3560–3571.
39. Toonen RF, de Vries KJ, Zalm R, et al. Munc18-1 stabilizes syntaxin 1, but is not essential for syntaxin 1 targeting and SNARE complex formation. *J Neurochem* 2005;93:1393–1400.
40. Toonen RF, Wierda K, Sons MS, et al. Munc18-1 expression levels control synapse recovery by regulating readily releasable pool size. *Proc Natl Acad Sci USA* 2006;103:18332–18337.

## SUPPORTING INFORMATION

Additional Supporting Information may be found in the online version of this article:

**Figure S1.** Expression analysis of Syn-1A, STXBPI, and Kv7.2 in CHO cells. Expression was tested by RT-PCR (A) and immunocytochemistry (B). (A) CHO cells were transfected with Syn-1A, STXBPI, or Kv7.2 (KCNQ2) plasmids independently or altogether (Triplex). Each gene was specifically amplified and was detectable only in the corresponding transfection or in the Triplex transfection. Amplification length of each gene is indicated in base pair (bp).

**Figure S2.** Syn-1A and STXBPI do not affect the surface expression of Kv7.2/Kv7.3 channels. (A) Kv7.2/Kv7.3 subunits were expressed alone or in combination with Syn-1A and STXBPI. Cells were treated with buffer alone (–) or

supplemented with sulfo-NHS-SS-biotin (+) before lysis; then membrane proteins and lysates were separated by SDS-PAGE and revealed for Kv7.2, Kv7.3, Syn-1A, STXBPI, or actin, as loading control. Molecular weight markers are shown on the left in kDa. (B) The ratios of surface/total Kv7 subunits were calculated and normalized to those in absence of Syn-1A and STXBPI. Bars represent mean ± SEM of four independent experiments. Syn-1A and STXBPI had no significant consequences on the surface expression of the Kv7.2/Kv7.3 channels, but Syn-1A significantly increased the protein expression of Kv7.2/Kv7.3 channels.

**Figure S3.** STXBPI does not affect the surface expression or protein levels of Kv7.2/Kv7.3 channels. (A) Kv7.2/Kv7.3 subunits were expressed alone or in combination with STXBPI. Cells were treated with buffer alone (–) or supplemented with sulfo-NHS-SS-biotin (+) before lysis; then membrane proteins and lysates were separated by SDS-PAGE and revealed for Kv7.2, Kv7.3, STXBPI, or actin, as loading control. Molecular weight markers are shown on the left in kDa. (B) The ratios of surface/total Kv7 subunits were calculated and normalized to those in absence of STXBPI. Bars represent mean ± SEM of four independent experiments. STXBPI had no significant consequences on the protein expression or surface expression of the Kv7.2/Kv7.3 channels.

**Table S1.** Primers used with the QuikChange II site-directed mutagenesis kit.

**Table S2.** Primers and PCR conditions for gene expression analysis.

**Table S3.** Functional analysis of homomeric Kv7.2 and heteromeric Kv7.2/Kv7.3 channels expressed in CHO cells. Effects of Syn-1A and/or STXBPI on V<sub>half</sub>, K slope factor, and current density (in pA/pF) measured in all the CHO cells expressing the homomeric Kv7.2 and heteromeric Kv7.2/Kv7.3 channels. All the values are represented as means ± SEM; \*comparison with Kv7.2 or Kv7.2/Kv7.3; §comparison with Kv7.2/Syn-1A (1:0.5) or Kv7.2/Kv7.3/Syn-1A (1:1:0.5); §comparison with Kv7.2/Syn-1A (1:1) or Kv7.2/Kv7.3/Syn-1A (1:1:1). \*/§/§ p < 0.05; \*/§§/§§ p < 0.01; \*\*/§§§/§§§§ p < 0.001; ND, not determined.